Resonance in the kidney system of rats

G. L. YU, Y. Y. LIN WANG, AND W. K. WANG
Biophysics Laboratory, Institute of Physics, Academia Sinica, Taipei 11529; Department of Electrical Engineering, National Taiwan University, Taipei 106; and Department of Physics, National Taiwan Normal University, Taipei, Taiwan 117, Republic of China

Yu, G. L., Y. Y. Lin Wang, and W. K. Wang. Resonance in the kidney system of rats. *Am. J. Physiol.* 267 (*Heart Circ. Physiol.* 36): H1544–H1548, 1994.—The pressure wave of the abdominal aorta and the flow wave of the renal artery were recorded simultaneously from a rat. The impedance of a kidney system that is derived by dividing the pressure of the corresponding frequency by that of the flow was studied in six rats. The data show that the system has two resonant frequencies, at the second and third harmonics. At the second harmonic, the pressure wave and fluid flow in a round trip through the branch of the kidney. Whereas it is difficult for the third harmonic flow to enter the kidney, it flows directly through the aorta. To obtain further proof, we compared the frequency components of the two flows measured simultaneously on the abdominal aorta and the renal artery and found the same result. The kidney, renal artery, and aorta combined show a coupled oscillation that is analogous to that of resonance circuits. The kidney vascular system exhibits a resonant frequency at the second harmonic of the heartbeat.

impedance; flow comparison; coupled oscillation

BLOOD PRESSURE and flow wave measurements are very important in studying the circulation system. The pressure-flow relationship represents the impedance as a function of the physical properties of the blood vessels (7, 10, 12, 14). It is usually used not only to explain the distortion or modulation of pressure waves but also to characterize the nature of different vascular beds.

Because each organ or vascular bed has its own specific shape, size, structure, and hemodynamic conditions, it will have its own properties of mechanics, which may be important to physiology. Some investigators (4, 5, 12, 14) have already noted this frequency dependence, but its importance has not been emphasized. Applying current reflection models, these investigators usually devote their attention to the reflection sites (2, 6, 12) and amount of reflection (7, 9). For example, Taylor's model (7, 8, 16, 17) of a vascular bed was a simple elastic tube with a closed distal end; O'Rourke (12, 13) proposed the asymmetric t-tube model to study the input impedance patterns of ascending aorta; and Liu et al. (6) and Burattini and colleagues (2) added complex loading to the terminal of the t tube. Even if their studies of the input impedance of the ascending aorta by these models may describe the whole vascular system, there is a trade-off of the individual characteristics of each vascular bed (2, 6, 13). Campbell et al. (3) pointed out further that the propagation constant and the effective length of the arterial system could be arbitrarily set and that the input impedance could be matched with many different models.

For obtaining information on organs or vascular beds, Wang et al. (18, 20) proposed the resonance model, which was based on the idea that the aorta and the closely attached organ can produce coupled oscillation. By this mechanism, the mechanical properties of the artery as well as the frequency dependence of the organ from the pressure wave on a peripheral artery can be studied (22, 23).

Several experiments have been performed to describe and support this model. A simulation of the circulation system using a pump, elastic tubes, and five different-sized balloons (with different natural frequencies) was performed. We found that the frequency composition of the pressure wave measured on the peripheral tube was different when the different balloons were clamped (18), and similar results were discovered when the left renal, the gastric, the splenic, and the superior mesenteric arteries each were clamped separately (18, 22, 23).

We have further simulated a short segment of the aorta and its side-branch organ using an elastic tube with a side-branch balloon (20). The following results were found: when the distance between the main tube and the side-branch balloon is large, their behavior can be explained by the simple reflection theory. However, when the distance is small enough, they cannot be regarded individually as reflective elements of the system, but together they form a coupled oscillator. The same result was found when we replaced the balloon with multigenerational branches.

These experiments indicated that the kidney system, which includes the kidney, renal artery, and aorta may be an example of a resonance element in animals (18–20, 22). In the present report, we measured the impedance of the kidney system of rats, comparing the abdominal flow with the renal flow in rats, and then used the resonant model to explain the data.

METHODS

Twelve Sprague-Dawley rats were anesthetized with urethan (1.2 mg/g body wt) and α-chloralose (12.5 μg/g body wt). Then, they were divided into two groups. In the first group, we measured the pressure wave in the abdominal aorta and flow wave in the renal artery. Cannulation from the root of the tail artery (arteria caudalis) to as close as possible to the entrance of renal artery was done by an intravenous catheter (Becton-Dickinson). The shape of the pressure pulse was recorded with a catheter-tip pressure transducer (RP-1500 Narco-Bio-System). This transducer responded up to 1,500 Hz. The assembly system was tested by the transient method (9). Its frequency response was uniform up to 60 Hz. The flow of renal artery was measured simultaneously with a pulsed Doppler flow system (Crystal Biotech VF-1, PD-20 module; 62.5-kHz pulse repetition frequency, 20 MHz, and 0.5-mm probe). In the second group, the flows in the renal artery and abdominal

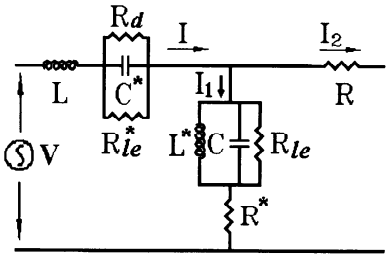

Fig. 1. Electrical analogs for a section of aorta with a side-branch organ: properties of kidney system (or other organ system) might be approached by this circuit. L, equivalent inductance in aorta; C, equivalent capacitance in aorta; R_{le}, leakage resistance of C; R and R_d, resistance and resistance of direct current in aorta, respectively; L*, equivalent inductance of side-branch organ; C^*, equivalent capacitance of side-branch organ; R^*, resistance of side-branch organ; R^*_{le}, the leakage resistance of C^*. I, I_1, and I_2 are currents.

aorta were simultaneously measured with two flowmeters. The aortic flow was measured below the renal arteries with a 1.25-mm probe.

These signals were connected to a simultaneous sample-and-hold panel AX753 (Axiom Technology, Taipei, Taiwan, R. O. C.) and then to an analog-to-digital converter AX5412, which is an interface card for a personal computer. The cards can amplify the amplitude of signals up to 8,000 times, sample them simultaneously (sampling rate = 4 kHz/channel), and convert them to digital data. Before these signals were analyzed, they went through a designed digital finite impulse response filter with Hamming windows (order = 200, cutoff frequency = 55 Hz, and sampling rate = 4 kHz) to filter out the high-frequency noise (11, 21).

We picked a period (both pressure and flow) between the two relatively lowest points to do discrete Fourier transform. The values of pressure and flow are divided to estimate impedance, and the values of two flows are subtracted to get a difference. The phase is calibrated by the time delay between the relatively lowest points of two simultaneous signals. A total of 12 periods of each rat was averaged. Because the amplitudes of flow and pressure decrease rapidly with the harmonic numbers (14) and because the resonance phenomenon was supposed to have an important effect on the lower harmonic components, we focused our attention only on the first six harmonics.

THEORY

We simulated a short segment of the aorta and its side-branch organ using an elastic tube with a side-branch balloon and proposed that the properties of these systems might be approached by an analogous electric circuit like that in Fig. 1 (20). In the circuit, the system has two resonance frequencies, ω_1 ($\sqrt{1/(L \cdot C^*)}$) and ω_2 ($\sqrt{1/(L^* \cdot C)}$), with ω_2 being higher than ω_1 from our previous observations (19), and where L is the equivalent inductance of the fluid (or blood) and C is the equivalent capacitance, imitating the behavior of the elastic wall of the tube, both in the aorta; L* and C^* are equivalent inductance and equivalent capacitance, respectively, in the side-branch organ (kidney).

The inductances and compliances of the circuit were not arbitrarily assigned; they were obtained by a three-step coupling. *1*) L and C belong to the tube (or the aorta), which behaves like a low-pass filter (9, 20). *2*) We treated the side-branch balloon in the same way as the first step with L* and C^*, coming from the side-branch balloon (or organ). *3*) Because the side-branch balloon behaves like a high-pass element of the main tube (9, 20, 22), C^* is coupled in series in the circuit and L* is coupled in parallel in the circuit. The combination of the first and second steps through the coupling mechanism was shown on Fig. 1 (20). The resistance of the renal artery is the source of the leakage resistance of C^* (R^*_{le}). R_d (similar to resistance R) is the resistance of direct current (DC) in the aorta flowing through the renal artery junction.

L and C^* are in series in the circuit: L is the inductance of this segment of aorta, and C^* is the part of the organ compliance (or the compliance of the balloon) that is coupled to the segment of aorta (or main elastic tube). This structure causes the low-impedance peak at ω_1. Because of the resistances R_d and R^*_{le} in the structure, the resonance peak is broadened. Because C^* belongs to the balloon (or organ), the current of the frequency ω_1 is a round-trip flow in and out of the balloon through R^*_{le}. The DC and the lower-frequency component ($< \omega_1$) may fill the C^* and travel along the tube through R_d.

L*, the part of organ inductance coupled to the aorta, and C, the compliance of the aorta, are in parallel in the circuit. The L*-C circuit makes the high impedance of this circuit at ω_2. C has leakage resistance R_{le}, and the amplitude of the impedance only shows a maximum. Because L* comes from the organ inductance, it is difficult for this frequency flow to enter the organ and it will flow directly through the aorta. If we compared the flows in the aorta to that in the branch artery, the amplitude difference of the impedance might show a maximum at ω_2.

These characteristics have been found in the balloon model. When the balloon was replaced by multigenerational branches, we obtained the same results. Moreover, we solved directly the coupled-oscillation equation with two degrees of freedom and still obtained the above results.

This frequency dependence has a very important consequence. It will filter out the pressure and flow waves to enter the side organs or to propagate continuously along the artery. This will facilitate the blood distribution and reduce the working load of the heart.

RESULTS

The average weight of the twelve rats was 353.75 ± 96.75 (SD) g. Average heart rate was 5.28 ± 0.43 Hz; average systolic and diastolic pressures of abdominal aortas were 115.52 ± 13.07 and 72.74 ± 10.78 mmHg, respectively; average peak velocities of blood flow in renal artery and abdominal aortas were 68.11 ± 18.12 and 92.59 ± 20.91 cm/s, respectively.

There are two groups of data in this report. Figures 2 and 3 are the samples from *groups 1* and *2*. In both figures, initial time (0 s) was the same on the *curves A* and *B*, and two signals were simultaneously recorded. For *group 1*, Fig. 2*A* is the pressure signal and Fig. 2*B* is

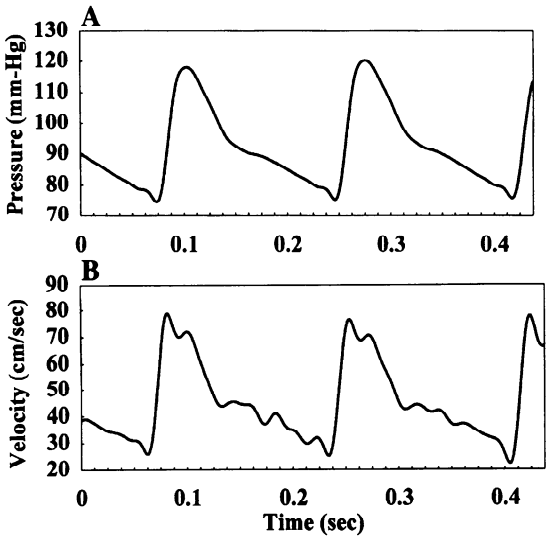

Fig. 2. Sample from *group 1* experiments. *A*: pressure signal of abdominal aorta. *B*: simultaneously recorded flow in renal artery. Impedance of kidney system was derived from these 2 signals.

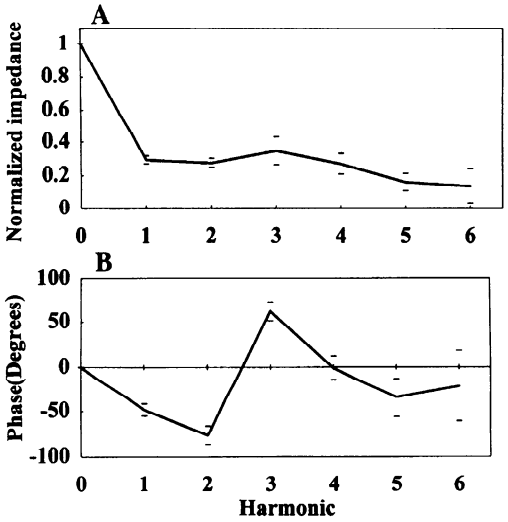

Fig. 4. Normalized impedance of the kidney system; bars are SD (n = 6). Normalized impedance was calculated by dividing each impedance harmonic by direct current (DC) impedance. Second and third harmonics are probably the resonant frequencies (ω_1 and ω_2).

the flow velocity; we can see that the flow pulse runs ahead of that of the pressure. For *group 2*, the flow of the abdominal aorta is shown in Fig. 3*A*, whereas Fig. 3*B* shows the renal flow. The systolic beginning of the two flows was at the same time.

Impedance curves, which are averaged from six rats are shown in Fig. 4. The normalized impedance was obtained by dividing each impedance harmonic by the constant term of the Fourier series (DC component). Error bars represent the standard deviation of the six rats. The positive value of phase means that flow lags behind pressure. There is a maximum in the normalized impedance in the third harmonic and a relative minimum in the second harmonic. For the phase, a negative maximum and a positive maximum can be seen in the second and third harmonics.

A comparison of the two flows is graphed in Fig. 5. The amplitude was normalized by the DC flow. Figure 5*A* is the difference of the two normalized amplitudes. A maximum at the third harmonic is shown. The phase difference is graphed in Fig. 5*B*. Its positive value shows that the phase of the flow in the renal artery runs ahead of that in the abdominal aorta [the positive value of phase difference, defined as the propagation constant $k \equiv 2\pi/\lambda$ (where λ is wavelength) in renal artery is larger]. We find that the renal flow runs ahead of the aortic after the second harmonic and that the two flows are almost in phase in the second harmonic.

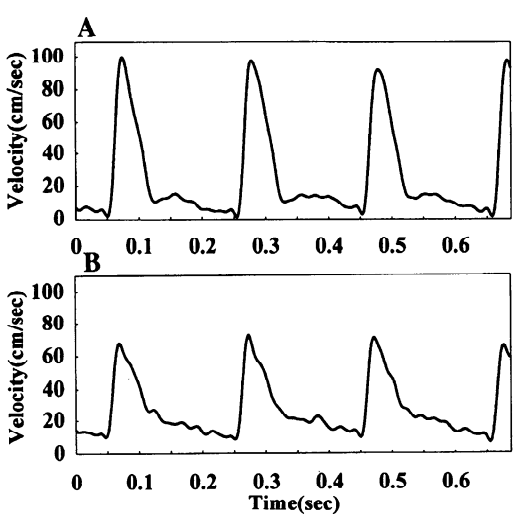

Fig. 3. Sample from *group 2* experiments. *A*: flow recorded in abdominal aorta. *B*: simultaneously recorded flow in renal artery.

DISCUSSION

We previously measured the flow of renal artery of rats with an EM (electromagnetic) flowmeter, but the dimension of the artery (~ 0.5 mm) is too small to obtain

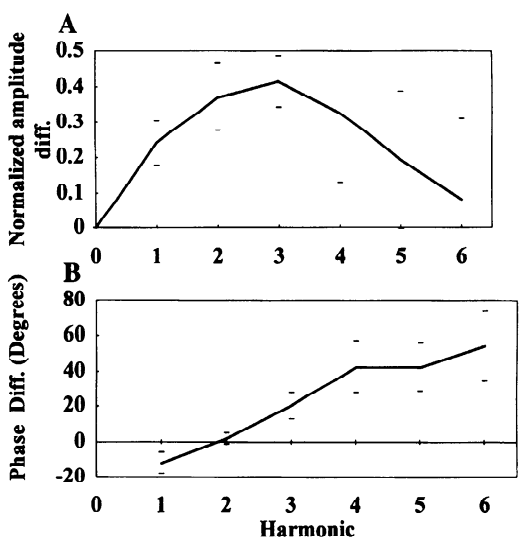

Fig. 5. Comparison of flows between abdominal aorta and renal artery: amplitudes were normalized by DC flow; differences of normalized amplitude and phase were derived by subtracting renal components from that of the aorta. Bars are SD (n = 6).

realistic data. Moreover, we compared flow data of the abdominal aorta of the rats with the EM and pulsed Doppler flowmeters in frequency domain. The differences of magnitude were within ±10% up to the fourth harmonic. The phases had large differences except at the first harmonic, and EM phases lagged behind the Doppler ones. Similar results were reported by Spencer et al. (15). However, from our data, the standard deviation of the EM was found to be four times higher than that of the Doppler. The small dimension (~1.25 mm) of rat aorta and the heavy EM probe may be the causes of the high EM standard deviation. Because the EM data are unreliable when the blood vessel is small (7), we used the Doppler flowmeter to measure the flow data.

Our data showed that the pressure and flow waves have good periodicity in normal state. Because the only frequencies in a periodic wave are its harmonics, all frequencies except those of the harmonics of heartbeat have very little energy and no importance in normal physiological state. If the resonance has any effects on physiology, then the band of the resonance frequencies of the organs must be very close to that of the harmonics of the heartbeat. That is why we devoted our attention only to the harmonics.

The system that includes a segment of aorta, renal artery, and kidney may be a good example of resonance. If the aorta and the closely attached kidneys have coupled oscillations, then the two resonance frequencies (ω_1 and ω_2) should be found. Our data show that the second and third harmonics may be the frequencies ω_1 and ω_2.

The modulus of impedance at the second harmonic is lower, so some component of flow should enter into renal artery (the side branch). Moreover, the phase of impedance at the second harmonic is close to the negative maximum, indicating that minimum power is delivered to it [power = current × voltage × cos(α)]. Furthermore, the two flows on renal artery and abdominal aorta are almost in phase, suggesting that they are the same flow. Consequently, this component of fluid flows in a round trip through the side branch with the pressure doing the same.

At the third harmonic, the modulus of impedance is a maximum; the phase of the impedance is near the positive maximum. The modulus difference of flows between the abdominal aorta and the renal artery is a maximum, with the phase of renal flow running ahead of that of the abdominal aorta. It is for these reasons we suggest that the flow of the third harmonic is separated into two flows and is more difficult to enter the renal artery.

The maximum and minimum may not be so clearly displayed on Fig. 3, but we have reason to argue that they exist in a physiological condition. The difference between the second and the third harmonic is distinguishable by a paired t-test ($P < 0.025$).

The model can also explain the experimental data of clamped renal artery in rats. When we temporarily clamped the left renal artery, the frequency variations of pressure wave above and including the second harmonic fell 30% or more (20, 22). From Fig. 1, C^* behaves as a high-pass element, and the components of the pressure wave above and including the second harmonic pass directly through C^*. If we clamped it, then the element would be lost and the components after the second harmonic should decrease.

The characteristics of frequency selectivity are very important to physiology. First, they help the pressure and flow of different frequencies enter the side organs or propagate continuously along the artery. This can reduce energy loss and the working load of the heart. Second, if the frequency dependence of the organ exists, then we may obtain some information about the organs by studying the output pressure wave on a peripheral artery (22, 23).

Address for reprint requests: W. K. Wang, Biophysics Lab., Institute of Physics, Academia Sinica, Nankang, Taipei, Taiwan 11529, R. O. C.

Received 14 June 1993; accepted in final form 9 May 1994.

REFERENCES

1. **Burattini, R., and S. D. Carlo.** Effective length of the arterial circulation determined in the dog by aid of a model of the systemic input impedance. *IEEE Trans. Biomed. Eng.* 1: 53–60, 1988.
2. **Burattini, R., G. G. Knowlen, and K. B. Campbell.** Two arterial effective reflective sites may appear as one to the heart. *Circ. Res.* 68: 85–99, 1991.
3. **Campbell, K. B., L. C. Lee, H. F. Frasch, and A. Noordergraaf.** Pulse reflection sites and effective length of the arterial system. *Am. J. Physiol.* 256 (*Heart Circ. Physiol.* 25): H1684–H1689, 1989.
4. **Latham, R. D., N. Weserhof, P. Sipkema, B. J. Rubal, P. Reuderink, and J. P. Murgo.** Regional wave travel and reflections along the human aorta: a study with six simultaneous micromanometric pressures. *Circulation* 72: 1257–1269, 1985.
5. **Li, J. K.-J., J. Melbin, and A. Noordergraaf.** Directional display of pulse reflection in the dog. *Am. J. Physiol.* 247 (*Heart Circ. Physiol.* 16): H95–H99, 1984.
6. **Liu, Z., S. Feng, and C. P. Y. Frank.** Impedance of arterial system simulated by viscoelastic t tubes terminated in windkessels. *Am. J. Physiol.* 256 (*Heart Circ. Physiol.* 25): H1087–H1099, 1989.
7. **McDonald, D. A.** *Blood Flow in Arteries* (2nd ed.). London: Arnold, 1974.
8. **McDonald, D. A., and M. G. Taylor.** The hydrodynamics of the arterial circulation. *Prog. Biophys. Biophys. Chem.* 9: 107–173, 1959.
9. **Milnor, W. R.** *Hemodynamics* (2nd ed.). Baltimore, MD: Williams & Wilkins, 1989.
10. **Milnor, W. R., and C. D. Bertran.** The relation between arterial viscoelasticity and wave propagation in the canine femoral artery in vivo. *Circ. Res.* 43: 870–879, 1978.
11. **Oppenheim, A. V., and R. W. Schafer** (Editors). *Discrete-Time Signal Processing.* Englewood Cliffs, NJ: Prentice-Hall, 1989, p. 444–488.
12. **O'Rourke, M. F.** Vascular impedance in studies of arterial and cardiac fuction. *Physiol. Rev.* 62: 570–623, 1982.
13. **O'Rourke, M. F.** Arterial stiffness, systolic blood pressure, and logical treatment of arterial hypertension. *Hypertension Dallas* 15: 339–347, 1990.
14. **Patel, D. J., F. M. Defreitas, and D. L. Fry.** Hydraulic input impedance to aorta and pulmonary artery in dogs. *J. Appl. Physiol.* 18: 134–140, 1963.

15. **Spencer, K. T., R. M. Lang, A. Neumann, K. M. Borow, and S. G. Shroff.** Doppler and electromagnetic comparisons of instantaneous aortic flow characteristics in primates. *Circ. Res.* 68: 1369–1377, 1991.
16. **Taylor, M. G.** An approach to an analysis of the arterial pulse wave. I. Oscillations in an attenuating line. *Phys. Med. Biol.* 1: 258–269, 1957.
17. **Taylor, M. G.** An approach to an analysis of the arterial pulse wave. II. Fluid oscillations in an elastic pipe. *Phys. Med. Biol.* 1: 321–329, 1957.
18. **Wang, W. K., Y. Y. Lo, T. L. Hsu, and Y. Y. L. Wang.** Resonance of organs with the heart. In: *Biomedical Engineering: An International Symposium*, edited by W. J. Young. New York: Hemisphere, 1989, p. 259–297.
19. **Wang, W. K., and Y. Y. L. Wang.** Biomedical engineering basis of traditional Chinese medicine. *Med. Prog. Technol.* 18: 191–197, 1992.
20. **Wang, Y. Y. L., S. L. Chang, Y. E. Wu, T. L. Hsu, and W. K. Wang.** Resonance, the missing phenomenon in hemodynamics. *Circ. Res.* 69: 246–249, 1991.
21. **Stanley, W. D., G. R. Dougherty, and R. Dougherty** (Editors). *Digital Signal Processing* (2nd ed.). Reston, VA: Reston Publishing, 1984, p. 215–242.
22. **Young, S. T., W. K. Wang, L. S. Chang, and T. S. Kao.** Specific frequency properties of renal and superior mesenteric arterial beds in rats. *Cardiovasc. Res.* 23: 465–467, 1989.
23. **Young, S. T., W. K. Wang, L. S. Chang, and T. S. Kao.** The filter properties of the arterial beds of organs in rats. *Acta Physiol. Scand.* 145: 401–406, 1992.